Climate Policy Uncertainty Regimes and Quantile Spillover Transmission across Green-Related Markets

Abstract

This study examines whether the magnitude, direction, and composition of spillovers across green-related and sustainable asset markets differ between low-, normal-, and high-climate policy uncertainty (CPU) regimes. Using daily data from May 2019 to March 2024, we analyze green technology, green bonds, aluminum, Polygon, water-related equities, and ESG-leading equities. CPU terciles are used to define the three regimes, while a quantile vector autoregressive connectedness framework measures total, directional, and pairwise spillovers across the lower tail, median, and upper tail. Baseline results show that connectedness among green-related markets is stronger at the tails than at the median and increases around major episodes of market stress. The regime analysis determines whether these variations reflect changes in aggregate connectedness, transmitter–receiver roles, or the composition of pairwise spillovers. High CPU is associated with lower total connectedness than low CPU across the lower tail, median, and upper tail, while directional and pairwise results indicate changes in network composition across regimes. The findings provide regime-conditioned information relevant to diversification assessment and extreme-return monitoring without implying a causal effect of CPU.

Keywords: Climate policy uncertainty; Green-related assets; extreme-return connectedness; Quantile connectedness; Uncertainty regimes

Amin Shakourloo[1*]
Department of Accounting and Finance, Faculty of Economics and Administrative Science, Cyprus International University, North Cyprus T.R. via Mersin 10 Turkey.

Asil Azimli[2]
Department of Accounting and Finance, Faculty of Economics and Administrative Science, Cyprus International University, North Cyprus T.R. via Mersin 10 Turkey.

1. Introduction

Uncertainty affects investment decisions, market valuations, and financing conditions (Bernanke, 1983; McDonald & Siegel, 1986; Baker et al., 2016; Gulen & Ion, 2016; Azimli, 2022, 2023). Climate policy uncertainty (CPU) is particularly relevant to green-related assets because changes in environmental regulation, carbon pricing, disclosure requirements, and public support for low-carbon investment may alter expected returns and risk exposures (Fuss et al., 2008; Treepongkaruna et al., 2023). Although climate risks can affect the wider financial system (Chenet et al., 2021), broader evidence also suggests that policy uncertainty may influence financial and macroeconomic conditions (Aastveit et al., 2017). Within this broader environment, green asset classes differ in market structure, liquidity, and sensitivity to climate-policy developments. CPU may therefore be associated with differences in both individual asset performance and cross-market shock transmission.

The equilibrium framework of Pástor et al. (2021) suggests that investors may accept lower expected returns from green-related assets because they value both their environmental characteristics and potential protection against climate risk. This perspective is consistent with broader evidence that climate-related risks are reflected in financial markets (Engle et al., 2020). Green-related assets may consequently attract greater demand when climate-policy uncertainty increases (Huynh & Xia, 2021; Pástor et al., 2021). Conversely, uncertain future policies may encourage firms to delay capital-intensive ESG equity investment and make financing more difficult **(**McDonald & Siegel, 1986; Bolton & Kacperczyk, 2021; Rubtsov et al., 2021). These competing mechanisms suggest that CPU may affect green markets heterogeneously rather than producing a uniform change in their connectedness.

Previous studies document substantial dependence and spillovers among green bonds, clean-energy equities, carbon markets, and other sustainable assets (Jin et al., 2020; Liu et al., 2021; Chatziantoniou et al., 2022; Naeem et al., 2023; Zhang & Umair, 2023). The evidence also suggests that green-market connectedness may become stronger during periods of market stress, potentially reducing diversification opportunities (Tiwari et al., 2022; Naeem et al., 2022; Urom, 2023; Wang et al., 2023). Other studies associate climate risk and CPU with the returns, volatility, and hedging characteristics of green assets (Bouri et al., 2022; Cepni et al., 2022; Dutta et al., 2023; Rehman et al., 2023). Özkan et al. (2024) and Tiwari et al. (2023) further examine connectedness under climate-related uncertainty, providing a foundation for investigating whether network structure differs across CPU regimes.

Nevertheless, evidence on whether green-asset networks are reconfigured across distinct CPU regimes remains limited. Recent studies examine connectedness under climate-related uncertainty but place less emphasis on regime-specific network composition (Gabauer et al., 2023; Özkan et al., 2024). Consequently, average connectedness may conceal differences in net transmitter–receiver roles and pairwise spillovers, particularly in the lower and upper tails. Accordingly, this study asks whether the magnitude, direction, and composition of green-asset spillovers differ across low-, normal-, and high-CPU regimes.

This study examines six markets represented by the S&P/TSX Renewable Energy and Clean Technology Index, S&P Green Bond Select Index, S&P GSCI Aluminum Index, Polygon, NASDAQ OMX Global Water Index, and S&P 500 ESG Leaders Index. The sample covers May 30, 2019, to March 28, 2024. Observations are classified into low-, normal-, and high-CPU regimes using terciles of the CPU distribution. We then apply the quantile vector autoregressive connectedness approach of Ando et al. (2022) and Chatziantoniou et al. (2022) to compare total, directional, and pairwise spillovers across the lower tail, median, and upper tail.

This study contributes to the literature in three respects. First, it examines CPU as a conditioning state of the green-asset network rather than only as a determinant of an aggregate connectedness index. Second, it combines CPU regimes with quantile connectedness to determine whether regime differences are concentrated in normal or extreme market conditions. Third, it considers a broad set of green-related markets with distinct economic and regulatory exposures, allowing changes in both system-wide connectedness and transmitter–receiver roles to be identified.

The baseline evidence indicates that connectedness is stronger at the distributional tails than at the median and rises around major periods of market stress. The regime analysis indicates lower TCI under high CPU across the three quantiles, alongside changes in selected transmitter–receiver and pairwise relationships. These findings may help investors assess regime-specific diversification opportunities and assist regulators in monitoring extreme-return connectedness. The results are interpreted as conditional associations and do not establish a causal effect of CPU.

The remainder of the paper is organized as follows. Section 2 reviews the related literature. Section 3 describes the data, CPU-regime classification, and methodology. Section 4 presents the empirical findings and robustness tests. Section 5 concludes.

2. Literature Review

Climate-related risks can influence asset prices by changing investors’ expectations, risk preferences, and portfolio allocations. Pástor et al. (2021) show that investors may accept lower expected returns from green-related assets because they value their environmental characteristics and potential protection against climate risk. Consistent with this view, Andersson et al. (2016) propose a decarbonized investment strategy for managing climate exposure, while Engle et al. (2020) construct portfolios designed to hedge climate-change news. Bolton and Kacperczyk (2021) further show that investors price exposure to carbon risk. These studies suggest that climate-related information can affect both asset valuations and the demand for ESG equity investment.

Climate-related risks can influence asset prices by changing investors' expectations, risk preferences, and portfolio allocations. Pástor et al. (2021) show that investors may accept lower expected returns from green-related assets because they value their environmental characteristics and potential protection against climate risk. Consistent with this view, Andersson et al. (2016) propose a decarbonized investment strategy for managing climate exposure, while Engle et al. (2020) develop portfolios designed to hedge climate-related news. Similar evidence is reported by Bua et al. (2024). Bolton and Kacperczyk (2021) document that investors price exposure to carbon risk, with related evidence reported by Ayed et al. (2024). Overall, the literature indicates that climate-related information is associated with asset valuations and ESG investment decisions (Vo et al., 2024).

A related literature examines whether green-related assets provide diversification or hedging benefits under climate risk. Jin et al. (2020) report that green bonds can hedge carbon-market risk. Arif et al. (2022) and Cepni et al. (2022) find that green bonds provide stronger protection against transition and physical climate risks than several conventional alternatives. Related comparisons between green and Islamic bonds also indicate differences in dependence structures across sustainable fixed-income assets (Ghaemi Asl et al., 2023). Dutta et al. (2023) document associations between climate risk and the returns and volatility of green-energy assets, while Arfaoui et al. (2024) show that ESG equity investment funds can offer diversification benefits under extreme climate-risk conditions. However, the performance of green-related assets is not necessarily uniform because green bonds, sustainable equities, transition-related commodities, and cryptocurrencies differ in their market structures and exposure to climate-policy developments.

Climate policy uncertainty adds another dimension to these relationships. Uncertainty concerning environmental regulation, carbon pricing, disclosure requirements, and green-investment support may influence green-related financial markets (Ongsakul et al., 2023; Sun et al., 2024). It may also influence investment decisions and expectations regarding future green-sector activity (McDonald & Siegel, 1986; Rubtsov et al., 2021; Du & Guo, 2023).

Empirical evidence also indicates heterogeneous market responses. Bouri et al. (2022) examine green and brown energy markets under CPU; Azimli (2023) and Azimli and Cek (2024) report heterogeneous responses across firms; Jin and Yu (2023) examine cryptocurrency markets, while Shahbaz et al. (2024) and Niu et al. (2023) document related transmission across commodity and financial markets. This heterogeneity implies that CPU may reconfigure the green-asset network rather than uniformly increase or decrease its connectedness.

Another strand of research examines spillovers among green and sustainable markets. Liu et al. (2021) identify dependence and risk transmission between green bonds and clean-energy markets, while Hanif et al. (2021) report similar interactions across sustainable financial assets. Tiwari et al. (2022) report that spillovers among green bonds, renewable-energy equities, and carbon markets vary during the COVID-19 period, with related evidence reported by Hoque et al. (2023). Using quantile-based methods, Chatziantoniou et al. (2022) find that connectedness among green bonds, green equities, sustainable investments, and clean energy differs across market conditions. Wang et al. (2023) document comparable distributional variation. Naeem et al. (2022) report stronger connections between green and conventional assets during extreme market states, while Ndubuisi and Urom (2023) and Urom (2023) document substantial integration involving environmentally oriented digital assets and green-related markets. Similar findings are reported by Karim et al. (2023) and Zhang et al. (2023. Collectively, these studies demonstrate that mean-based connectedness measures may conceal important tail-risk dynamics.

More recent research connects CPU with green-market spillovers. Wang et al. (2023) examine connectedness among CPU, energy, green bonds, and carbon markets, while Özkan et al. (2024) use a quantile-VAR framework to study the role of CPU in clean-energy and sustainable-market connectedness. Nevertheless, limited evidence is available on whether the magnitude, direction, and composition of green-asset spillovers differ systematically across distinct CPU regimes. In particular, an average relationship between CPU and total connectedness may conceal changes in pairwise spillovers or shifts in the identities of net transmitters and receivers.

This study addresses this gap by classifying observations into low-, normal-, and high-CPU regimes and comparing total, directional, and pairwise quantile connectedness across them. By combining CPU regimes with lower-tail, median, and upper-tail estimates, the analysis evaluates whether green-asset networks become more integrated or fragmented as policy uncertainty changes and whether individual markets switch their shock-transmission roles. This regime-conditioned perspective extends the existing literature from estimating an average CPU–connectedness relationship toward examining changes in the structure of the green-asset network.

3.1. Data

The study examines connectedness across six green-related and sustainable markets: renewable-energy technology, green bonds, a transition-related metal, an energy-efficient cryptocurrency, water-related equities, and ESG equities. Green technology is represented by the S&P/TSX Renewable Energy and Clean Technology Index (GT), green bonds by the S&P Green Bond Select Index (GB), and transition-related metal by the S&P GSCI Aluminum Index (GM). Polygon in US dollars represents energy-efficient cryptocurrency (GC), the NASDAQ OMX Global Water Index represents green water (GW), and the S&P 500 ESG Leaders Index represents ESG equity investment (GI). These assets capture different segments of sustainable finance and differ in liquidity, market structure, and exposure to climate-policy developments.

Aluminum is treated as a transition-related commodity because of its extensive use in renewable-energy infrastructure, including solar panels, wind turbines, electricity networks, and electric vehicles. It is not classified as an intrinsically green asset. Polygon is treated as an energy-efficient digital-asset proxy because its proof-of-stake architecture has substantially lower direct energy requirements than proof-of-work cryptocurrency networks. Nevertheless, neither aluminum nor Polygon is exclusively linked to sustainable activity. The analysis therefore uses the broader term "green-related markets". The remaining indices represent green technology, labeled green bonds, water-related businesses, and companies with relatively strong ESG characteristics. Price data are obtained from S&P Dow Jones Indices and Investing.com, as summarized in Table 1.

Climate policy uncertainty is measured using the CPU index developed by Gavriilidis (2021), which has been adopted in recent empirical studies (Azimli, 2023; Ongsakul et al., 2023; Azimli & Cek, 2024). The index is constructed from newspaper coverage of uncertainty associated with climate policy, environmental regulation, emissions, and renewable energy. Because the original CPU index is available monthly, the baseline analysis assigns each monthly CPU observation to all trading days within the corresponding month. This preserves the information frequency of the original index and avoids introducing artificial daily variation.

The natural logarithm of CPU is used to reduce scale differences and potential heteroscedasticity (Olasehinde-Williams & Özkan, 2023). The sample covers May 30, 2019, to March 28, 2024, based on the joint availability of the asset series. All observations are aligned to common trading dates. Asset returns are calculated as:

$$R_{i,t} = 100 \times \ln\left(\frac{P_{i,t}}{P_{i,t-1}}\right), \tag{1}$$

where $P_{i,t}$ is the price of asset $i$on day t. The return series are used in the quantile-connectedness estimations, while the logged CPU series is used to define the uncertainty regimes.

To examine whether the green-asset network changes with CPU, the observations are divided into three regimes using CPU terciles:

$$CPURegime_t = \begin{cases} Low, & CPU_t \leq Q_{0.33}, \\ Normal, & Q_{0.33} < CPU_t \leq Q_{0.67}, \\ High, & CPU_t > Q_{0.67}, \end{cases} \tag{2}$$

where $Q_{0.33}$ and $Q_{0.67}$ denote the 33rd and 67th percentiles of the logged CPU distribution. This classification provides a transparent separation of relatively low, normal, and high uncertainty observations while retaining sufficient observations for regime-conditioned comparison. Regime-based classification has been widely applied to examine differences across market states (Ang & Bekaert, 2002). The rolling QVAR model is estimated over the chronologically ordered full sample. The resulting daily connectedness measures are subsequently grouped according to contemporaneous low-, normal-, and high-CPU regimes to compare total, directional, and pairwise connectedness across the lower tail, median, and upper tail.

Table 1. Variable definitions

Symbol	Market	Proxy	Source
GT	Renewable-energy technology	S&P/TSX Renewable Energy and Clean Technology Index	S&P DJI
GB	Green bonds	S&P Green Bond Select Index	S&P DJI
GM	transition-related metal	S&P GSCI Aluminum Index	S&P DJI
GC	energy-efficient cryptocurrency	Polygon/USD	Investing.com
GW	Water-related equities	NASDAQ OMX Global Water Index	Investing.com
GI	ESG equities	S&P 500 ESG Leaders Index	S&P DJI
CPU	Climate policy uncertainty	Climate Policy Uncertainty Index	Gavriilidis (2021); PolicyUncertainty.com

3.2. Methodology

3.2.1. Quantile connectedness framework

We employ the quantile vector autoregressive (QVAR) connectedness framework developed by Ando et al. (2022) and Chatziantoniou et al. (2022), which extends earlier quantile connectedness applications (Chatziantoniou et al., 2021). Similar connectedness frameworks have been applied in recent financial-network studies (Antonakakis et al., 2020; Gabauer et al., 2023). Unlike mean-based VAR models, QVAR estimates connectedness at different points of the conditional return distribution, allowing spillovers to be evaluated under bearish, normal, and bullish market conditions.

For quantile τ, the QVAR model is specified as:

$$Q_\tau(R_t \mid \mathcal{F}_{t-1}) = c(\tau) + \sum_{j=1}^{p} \Phi_j\,(\tau) R_{t-j} \tag{3}$$

$$R_t = c(\tau) + \sum_{j=1}^{p} \Phi_j\,(\tau) R_{t-j} + \varepsilon_t(\tau), \tag{4}$$

Where $R_t$is the vector of green-asset returns, $c(\tau)$ is the intercept vector, $\Phi_j(\tau)$ contains the quantile-specific coefficients, p is the lag order, and $\varepsilon_t(\tau)$ is the error vector. The lag order is selected using the Bayesian Information Criterion.

Where:

$$Q_\tau\,(\varepsilon_t(\tau) \mid \mathcal{F}_{t-1}) = 0 \tag{5}$$

The QVAR is transformed into its moving-average representation, from which the generalized forecast-error variance decomposition (GFEVD) is obtained (Koop et al., 1996; Pesaran & Shin, 1998). The normalized variance share is:

$$\tilde{\theta}_{ij}^{g}(H,\tau) = \frac{\theta_{ij}^{g}(H,\tau)}{\sum_{j=1}^{N} \theta_{ij}^{g}(H,\tau)}, \tag{6}$$

Where $\tilde{\theta}_{ij}^{g}(H,\tau)$ measures the proportion of the H-step-ahead forecast-error variance of asset $i$attributable to shocks from asset $j$at quantile τ.

3.2.2. Connectedness measures

Total quantile connectedness measures the overall proportion of forecast-error variance arising from cross-market shocks:

$$TCI(\tau) = \frac{1}{N} \sum_{i=1}^{N} \sum_{\substack{j=1 \\ j \neq i}}^{N} \tilde{\theta}_{ij}^{g}(H,\tau) \times 100. \tag{7}$$

Directional connectedness received by asset $i$from all other assets is:

$$FROM_i(\tau) = \sum_{\substack{j=1 \\ j \neq i}}^{N} \tilde{\theta}_{ij}^{g}(H,\tau) \times 100, \tag{8}$$

While directional connectedness transmitted by asset $i$to the remaining markets is:

$$TO_i(\tau) = \sum_{\substack{j=1 \\ j \neq i}}^{N} \tilde{\theta}_{ji}^{g}(H,\tau) \times 100. \tag{9}$$

Net directional connectedness is calculated as:

$$NET_i(\tau) = TO_i(\tau) - FROM_i(\tau). \tag{10}$$

A positive NET_i identifies asset $i$as a net shock transmitter, whereas a negative value identifies it as a net receiver. Pairwise directional connectedness is also examined to determine which bilateral relationships account for changes in the overall network:

$$NPDC_{ij}(\tau) = \tilde{\theta}_{ji}^{g}(H,\tau) - \tilde{\theta}_{ij}^{g}(H,\tau). \tag{11}$$

A positive value indicates that asset $i$is a net transmitter of shocks to asset j.

3.2.3. CPU-regime comparison

Connectedness is estimated at the lower-tail ($\tau = 0.05$), median ($\tau = 0.50$), and upper-tail ($\tau = 0.95$) quantiles. The baseline dynamic model uses a 200-trading-day rolling window, a 20-day forecast horizon, and one lag. The longer window provides more stable estimation at the 0.05 and 0.95 quantiles while retaining sufficient time variation.

To preserve the chronological structure of the return series, the rolling QVAR is first estimated over the full sample. Each daily connectedness estimate is then assigned to the contemporaneous low-, normal-, or high-CPU regime. Regime-conditioned connectedness is calculated as:

$$\bar{C}_{r,\tau} = \frac{1}{T_r} \sum_{t:Regime_t = r} C_t(\tau), \tag{12}$$

$$\Delta C_{r,s,\tau} = \bar{C}_{r,\tau} - \bar{C}_{s,\tau}, r \neq s \tag{13}$$

where $C_t(\tau)$ represents the relevant total, directional, or pairwise connectedness measure, $r \in \{Low, Normal, High\}$, and $T_r$is the number of observations in regime r.

For each quantile, the analysis compares total connectedness, directional spillovers, net transmitter–receiver positions, and pairwise directional connectedness across the three CPU regimes. Regime differences are calculated for the high–low, high–normal, and normal–low comparisons. Statistical inference is based on moving-block bootstrap confidence intervals, preserving the serial dependence and overlapping-window structure of the connectedness estimates. Bootstrap p-values are adjusted using the Benjamini–Hochberg procedure where multiple asset-level or pairwise comparisons are conducted. The results identify conditional differences across CPU regimes and are not interpreted as causal effects of CPU.

This procedure avoids treating nonconsecutive observations as adjacent time-series observations, which could arise if the sample were partitioned by CPU terciles before estimating the QVAR. The subsequent analysis compares CPU regimes with respect to total quantile connectedness, lower-tail, median, and upper-tail connectedness, net transmitter–receiver positions, and pairwise directional spillovers.

The moving-block bootstrap uses [insert block length] trading-day blocks and 1,000 replications. Statistical significance is evaluated using 95% confidence intervals. Benjamini–Hochberg adjusted p-values are reported for asset-level and pairwise comparisons.

3.2.4. Robustness tests

The robustness analysis considers alternative rolling-window lengths of 150 and 250 trading days relative to the 200-day baseline and a shorter 10-day forecast horizon relative to the 20-day baseline. The sensitivity of the regime classification is examined using a two-regime median split of logged CPU. In addition, the median QVAR results are compared with the generalized mean-based connectedness approach of Diebold and Yilmaz (2012). These specifications assess whether the direction and relative pattern of the High–Low CPU connectedness differences remain broadly consistent with the baseline estimates.

4. Findings and Discussion

Table 2 presents the descriptive statistics for the six green-asset returns and logged CPU. Mean returns are close to zero for most assets, while green cryptocurrency (GC) has the highest variance, followed by green technology (GT) and green metal (GM). GT, GC, GW, GI, and CPU exhibit significant negative skewness, whereas the skewness of GB and GM is not statistically significant. All series display significant excess kurtosis and reject normality under the Jarque–Bera test. The weighted portmanteau statistics (Fisher & Gallagher, 2012) indicate serial dependence for most series and significant dependence in squared observations for all series. These distributional features support examining connectedness beyond the conditional mean.

Table 2. Descriptive statistics

	GT	GB	GM	GC	GW	GI	CPU
Mean	-0.015	-0.008	0.022	0.314	0.041	0.061	2.262
Med	0.018	-0.006	0.000	0.034	0.084	0.087	2.303
Max	9.990	2.516	6.090	45.188	9.056	9.543	2.958
Min	-13.290	-2.962	-6.936	-73.616	-10.872	-12.985	1.254
Var	2.672	0.265	1.958	73.428	1.425	1.907	0.085
Ske	-0.790*	-0.085	-0.019	-0.321*	-0.646*	-0.795*	-0.588*
p	0.000	0.225	0.788	0.000	0.000	0.000	0.000
Ex.K	11.120*	3.448*	2.027*	11.258*	12.634*	14.135*	0.942*
p	0.000	0.000	0.000	0.000	0.000	0.000	0.000
JB	6376.504*	602.456*	207.811*	6426.939*	8152.302*	10225.936*	114.670*
p	0.000	0.000	0.000	0.000	0.000	0.000	0.000
Q(10)	23.889*	41.485*	10.367***	8.152	62.826*	128.624*	5450.024*
p	0.000	0.000	0.059	0.159	0.000	0.000	0.000
Q^2(10)	1031.433*	192.988*	154.185*	54.486*	711.482*	1044.372*	5463.591*
p	0.000	0.000	0.000	0.000	0.000	0.000	0.000

Notes: $Q(10)$and $Q^2(10)$ denote the weighted portmanteau statistics for the series and their squares, respectively. * and *** indicate significance at the 1% and 10% levels.

Stationarity is assessed using the Augmented Dickey–Fuller (ADF) (Dickey & Fuller, 1979) and Phillips–Perron (PP) tests (Phillips & Perron, 1988). The QADF and QPP results in Figures 1 and 2 reject the unit-root null for the green-asset returns and logged CPU across the examined quantiles. The transformed series are therefore treated as stationary for the subsequent connectedness analysis.

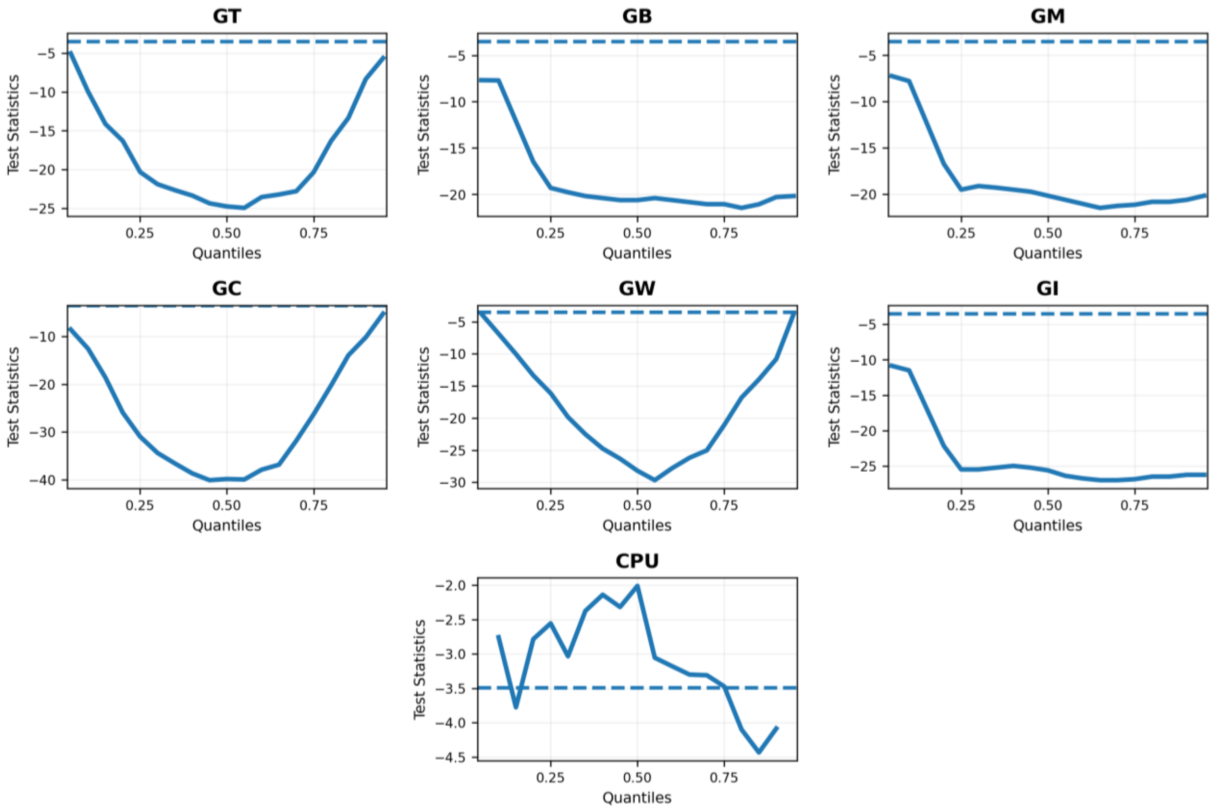

Fig 1. Quantile ADF unit-root test results

Note: GT, GC, GW, and CPU are re-estimated from the raw data used in the revised analysis. For GB, GM, and GI, the corresponding QADF results from the original analysis are retained because the underlying raw series were unavailable for the present re-estimation. The dashed line denotes the 1% critical value.

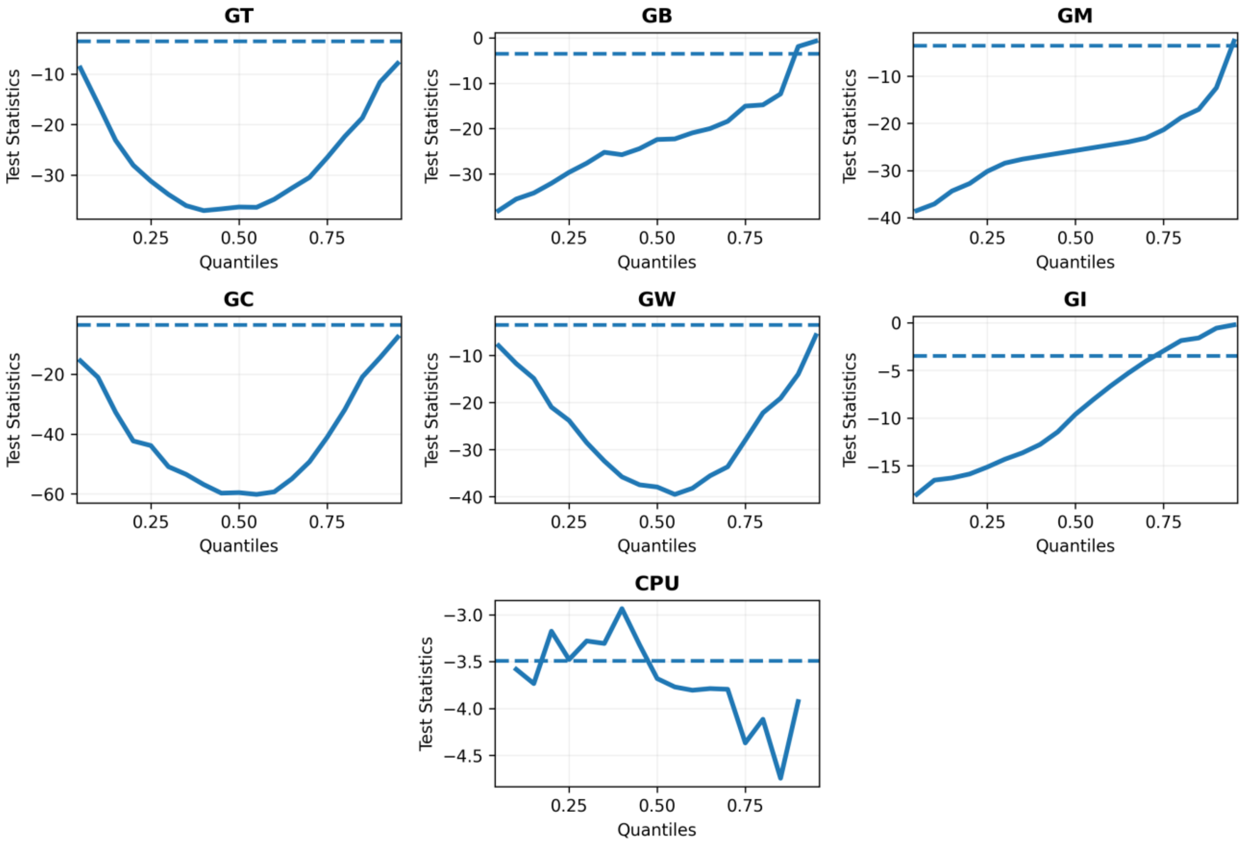

Fig 2. Quantile PP unit-root test results
Note: The dashed line represents the critical value at the 1% level. The results indicate rejection of the unit-root null across the examined quantiles for the green-asset return series. CPU exhibits comparatively weaker rejection at some quantiles. GT, GC, GW, and CPU are re-estimated from the available raw data, while GB, GM, and GI retain the corresponding results from the original analysis.

Table 3 reports the BDS test results. The i.i.d. null is rejected across embedding dimensions two to six for the green-asset returns. CPU also shows evidence against the i.i.d. null, although the result is weaker at the second embedding dimension. These patterns are consistent with nonlinear dependence and provide motivation for the quantile-based specification (Broock et al., 1996; Özkan et al., 2024).

Table 3. BDS Test Outcomes

	GT	GB	GM	GC	GW	GI	CPU
2nd ed	8.738*	9.144*	4.875*	7.835*	11.100*	8.942*	2.221
p	0.000	0.000	0.000	0.000	0.000	0.000	0.026
3rd ed	10.801*	10.311*	6.457*	10.821*	12.966*	12.567*	3.564*
p	0.000	0.000	0.000	0.000	0.000	0.000	0.000
4th ed	12.044*	11.097*	7.619*	12.614*	13.744*	14.928*	4.326*
p	0.000	0.000	0.000	0.000	0.000	0.000	0.000
5th ed	13.001*	12.222*	8.348*	14.031*	14.166*	16.848*	4.349*
p	0.000	0.000	0.000	0.000	0.000	0.000	0.000
6th ed	13.600*	13.431*	9.051*	15.242*	14.492*	18.835*	4.415*
p	0.000	0.000	0.000	0.000	0.000	0.000	0.000

Note: ed denotes embedding dimension. * indicates significance at the 1% level. GT, GC, GW, and CPU are re-estimated from the available raw data; GB, GM, and GI retain the corresponding results from the original analysis. The CPU statistic at embedding dimension 2 is significant at the 5% rather than the 1% level.

The BDS results indicate departures from i.i.d. behavior across the asset-return series. The newly estimated GT, GC, and GW statistics remain significant at the 1% level across all embedding dimensions. CPU also rejects the i.i.d. null, although its second-dimension result is significant only at the 5% level. Overall, the results are consistent with nonlinear dependence and support the use of a quantile-based connectedness framework (Broock et al., 1996; Nishiyama et al., 2011).

Table 4 reports the parameter-stability tests. The results suggest some instability for GT and CPU, whereas the evidence is weaker for GC and GW. Together with the retained results for the remaining series, the tests indicate heterogeneous stability patterns across the system, consistent with allowing connectedness to vary over time and across CPU regimes.

Table 4. Parameter-stability test results

	GT	**GB**	**GM**	**GC**	**GW**	**GI**	**CPU**
Max. LR-F	10.987**	6.809**	3.423	4.755	4.243	26.765*	14.973*
p	0.021	0.021	0.310	0.260	0.327	0.000	0.006
Exp. LR-F	2.220**	1.690**	0.436	0.715	0.304	9.742*	4.826*
p	0.043	0.041	0.601	0.300	0.630	0.000	0.005
Ave. LR-F	2.634***	2.776**	0.747	1.156	0.543	13.288*	4.448**
p	0.067	0.024	0.561	0.287	0.600	0.000	0.017

Note: Max. LR-F, Exp. LR-F, and Ave. LR-F denote the maximum, exponential, and average LR-F statistics, respectively. *, **, and *** indicate significance at the 1%, 5%, and 10% levels. GT, GC, GW, and CPU are re-estimated from the available raw data; GB, GM, and GI retain the corresponding results from the original analysis.

The newly estimated results provide some evidence of parameter instability for GT and CPU. GT is significant under the maximum and exponential tests and marginally significant under the average test, while CPU is significant across all three measures. GC and GW do not reject parameter stability in the new estimates. Overall, the mixed stability patterns are consistent with examining time-varying connectedness and regime-conditioned differences rather than assuming constant relationships throughout the sample (Andrews, 1993; Hansen, 1997).

Finally, Figure 3 presents the quantile–quantile plots. Departures from the reference line are more visible toward the tails for several asset returns, suggesting deviations from normality. This pattern is consistent with the distributional features reported above and provides additional motivation for examining connectedness across different return quantiles.

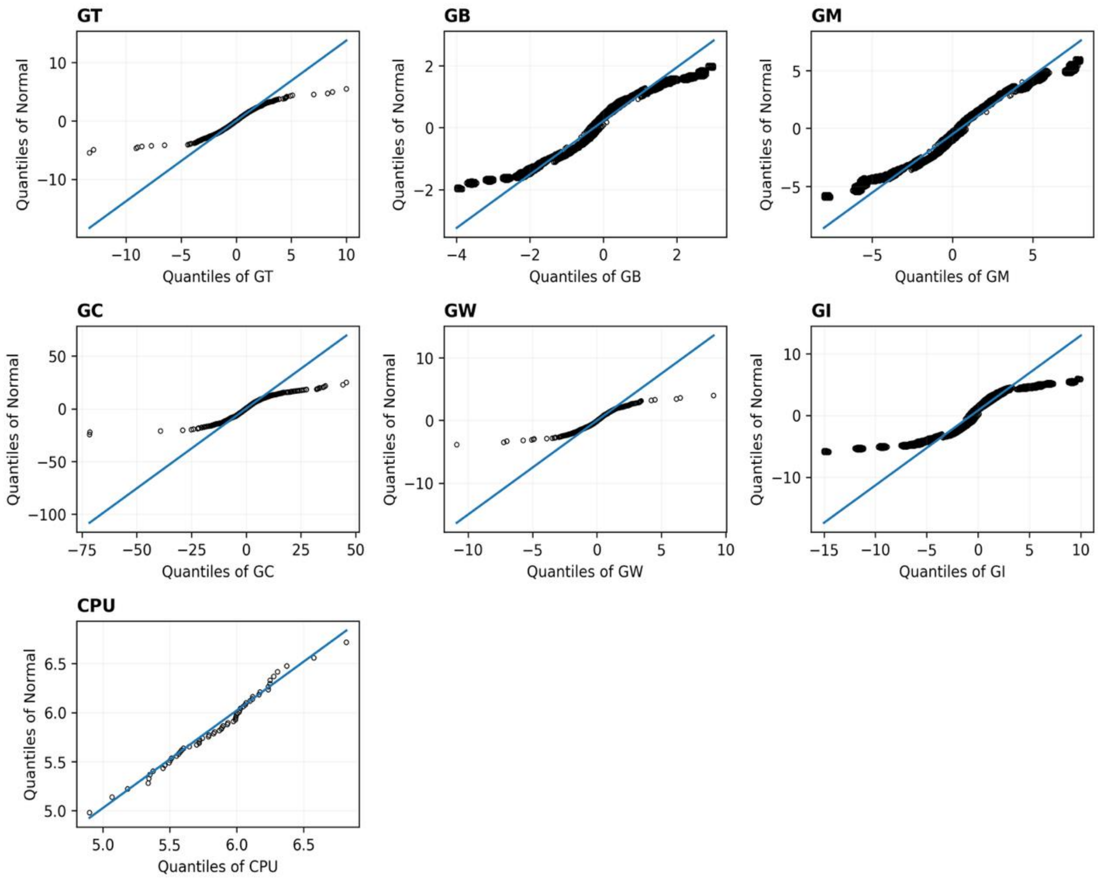

Fig 3. Quantile–quantile plots for green-asset returns and CPU

Note: The reference line represents the fitted normal benchmark. Departures from the line indicate deviations from normality. GT, GC, GW, and CPU are reconstructed from the available raw data, while GB, GM, and GI retain the corresponding empirical patterns from the original analysis and are redrawn for consistency.

The plots show comparatively larger departures from the normal benchmark in the tails of several series. GC displays particularly pronounced tail deviations, while the remaining asset returns exhibit varying degrees of non-normality. CPU shows a different distributional pattern from the return series. Together with the BDS and stability diagnostics, these results are consistent with using a quantile-based framework without implying a uniform distributional structure across the variables.

4.2.1 Baseline Total Connectedness

We first estimate the baseline QVAR connectedness model over the full sample before conditioning the estimates on CPU regimes. The revised specification uses a 200-day rolling window, a 20-day forecast horizon, and one lag selected by the Bayesian Information Criterion. Figure 4 presents dynamic total connectedness across the conditional return distribution. Connectedness is generally stronger in the tails, particularly around the lower and upper extremes, than around the median. The lower- and upper-tail patterns are broadly comparable, although symmetry is not imposed. This distributional variation is consistent with more limited diversification opportunities across the six green-related markets during relatively large negative and positive return movements.

Higher connectedness is visible during parts of the COVID-19 pandemic, the Russia–Ukraine war, and the Israel–Hamas war. Similar patterns have been reported during periods of elevated market uncertainty (Wang et al., 2022; Mandaci et al., 2023). The visual correspondence is also broadly consistent with discussions of investor uncertainty and portfolio rebalancing in the connectedness literature (Salisu & Vo, 2020; Mensi et al., 2022). Since the analysis does not formally evaluate event effects, these observations should be interpreted as descriptive rather than causal.

Overall, the baseline estimates indicate substantial variation in green-asset connectedness across both time and return quantiles. This provides the full-sample benchmark for the subsequent analysis of whether network configurations differ across low-, normal-, and high-CPU regimes, including differences in aggregate connectedness, transmitter–receiver positions, and pairwise spillovers.

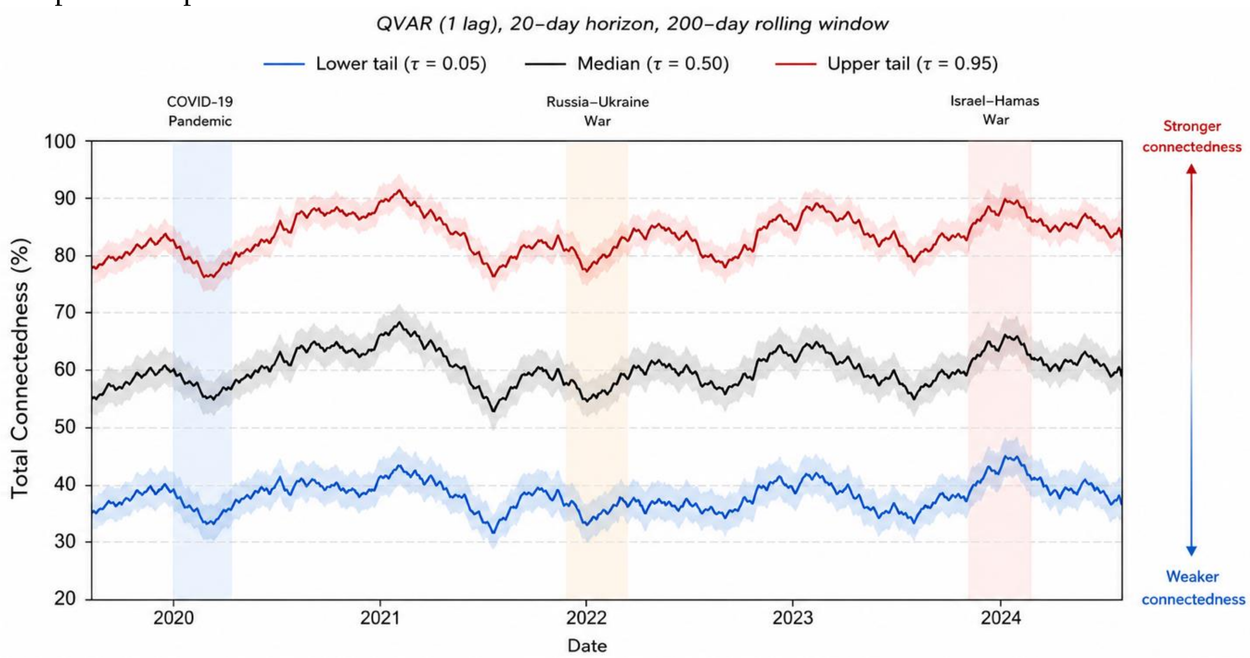

Fig 4. Dynamic total quantile connectedness across green asset markets

Note: The figure reports rolling total quantile connectedness for GT, GB, GM, GC, GW, and GI. Solid lines represent point estimates, while shaded areas indicate ±1 standard error obtained from a moving-block bootstrap with 1,000 replications. Estimates use a 200-day rolling window, one lag selected by BIC, and a 20-day forecast horizon. Lower-tail, median, and upper-tail connectedness correspond to $\tau =$ 0.05, 0.50, and 0.95, respectively. Higher values indicate stronger system-wide connectedness across the six green-related markets.

Figure 4 shows that total connectedness varies across time and return quantiles. Connectedness is generally higher in the lower and upper tails than around the median. Relatively higher connectedness is also visible during parts of several broad market-stress periods. This pattern is broadly consistent with previous quantile connectedness evidence (Mandaci et al., 2023; Khan et al., 2023; Özkan et al., 2024). These baseline results provide a benchmark for the subsequent CPU-regime analysis.

4.2.2 Baseline Net Directional Connectedness

Figure 5 presents the baseline net directional quantile connectedness. Net connectedness is measured as the shocks transmitted by each market to the remaining system minus the shocks received from other markets. Positive values indicate a net-transmitter position, whereas negative values indicate a net-receiver position (Mandaci et al., 2023).

The estimates indicate heterogeneous network roles across markets, time, and return quantiles. GW and GI generally appear on the transmitter side of the network, whereas GB, GM, and GC more frequently occupy receiver positions. GT exhibits greater variation, moving between transmitter and receiver positions over the sample. The intensity and persistence of these positions also vary across the conditional return distribution, suggesting that market roles are not uniform across states.

GB's predominantly negative net connectedness is consistent with relatively greater reception of shocks from the remaining markets. This position alone does not imply hedging or diversification benefits, since such conclusions would require portfolio-based evidence. Nevertheless, the pattern is broadly consistent with earlier studies reporting distinctive dependence and diversification characteristics for green bonds (Naeem et al., 2021; Cepni et al., 2022; Tiwari et al., 2022).

Taken together, the full-sample estimates suggest that transmitter–receiver positions vary across both time and quantiles. They provide the baseline against which the subsequent Low–Normal–High CPU regime analysis evaluates whether network roles systematically reconfigure across climate-policy-uncertainty conditions.

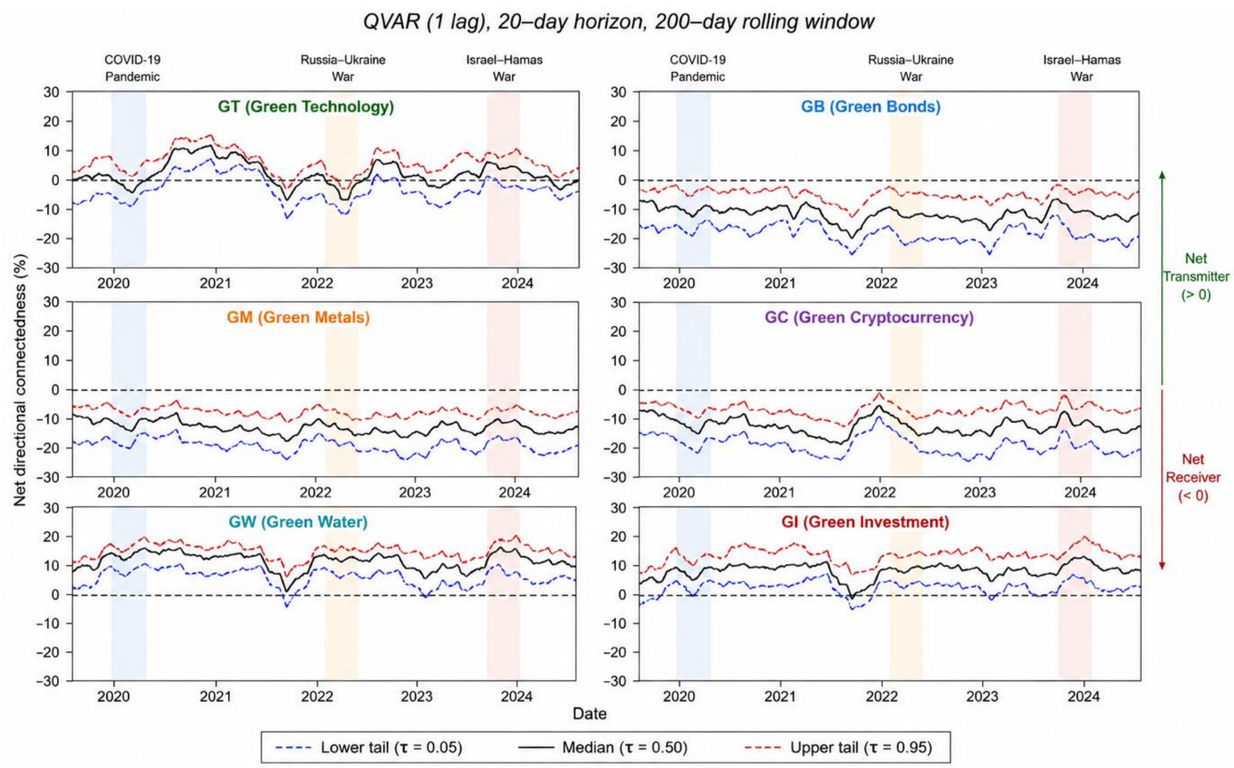

Fig 5. Dynamic net directional quantile connectedness across green-related markets

Note: The figure reports net directional connectedness for GT, GB, GM, GC, GW, and GI at the lower-tail ($\tau = 0.05$), median ($\tau = 0.50$), and upper-tail ($\tau = 0.95$) quantiles. Positive values indicate net-transmitter positions and negative values indicate net-receiver positions. The horizontal zero line separates the two network roles. Estimates use a 200-day rolling window, one lag selected by BIC, and a 20-day forecast horizon.

GW and GI display predominantly positive net positions, while GB, GM, and GC are more frequently net receivers, a pattern broadly consistent with Naeem et al. (2023). GT shows comparatively greater switching between the two positions. The variation across time and quantiles is consistent with evidence that transmitter–receiver roles may differ across market conditions (Wang et al., 2023) and provides the benchmark for the subsequent CPU-regime analysis.

GB remains predominantly a net receiver throughout the sample. This pattern is broadly consistent with earlier evidence that green bonds often occupy a distinct position within connectedness networks and may exhibit different dependence characteristics from other green-related assets (Cepni et al., 2022; Naeem et al., 2021; Tiwari et al., 2022). The baseline results provide the reference point for the subsequent CPU-regime comparison.

4.3. Connectedness across CPU Regimes

4.3.1. Total connectedness

Table 5 compares total connectedness across CPU regimes. TCI is lower under high CPU at all three quantiles, with the largest High–Low difference in the upper tail. Block-bootstrap tests indicate significant differences across all three quantiles.

Table 5. Total quantile connectedness across CPU regimes

Quantile	Low CPU	Normal CPU	High CPU	High–Low difference	Bootstrap p-value
Lower tail ($\tau = 0.05$)	42.888	43.655	36.423	−6.465	0.001
Median ($\tau = 0.50$)	36.824	39.213	31.411	−5.413	0.001
Upper tail ($\tau = 0.95$)	41.763	43.919	34.252	−7.511	0.001

Note: Entries report average rolling TCI by CPU regime. CPU regimes are defined by the 33rd and 67th percentiles of logged CPU. Estimates use a 200-day rolling window, one lag, and a 20-day forecast horizon. P-values are based on 1,000 moving-block bootstrap replications.

High CPU is associated with lower connectedness across all three quantiles. The difference is largest in the upper tail (−7.511 percentage points), while normal CPU records the highest average TCI. The results are consistent with regime-dependent variation in system-wide connectedness rather than a causal CPU effect.

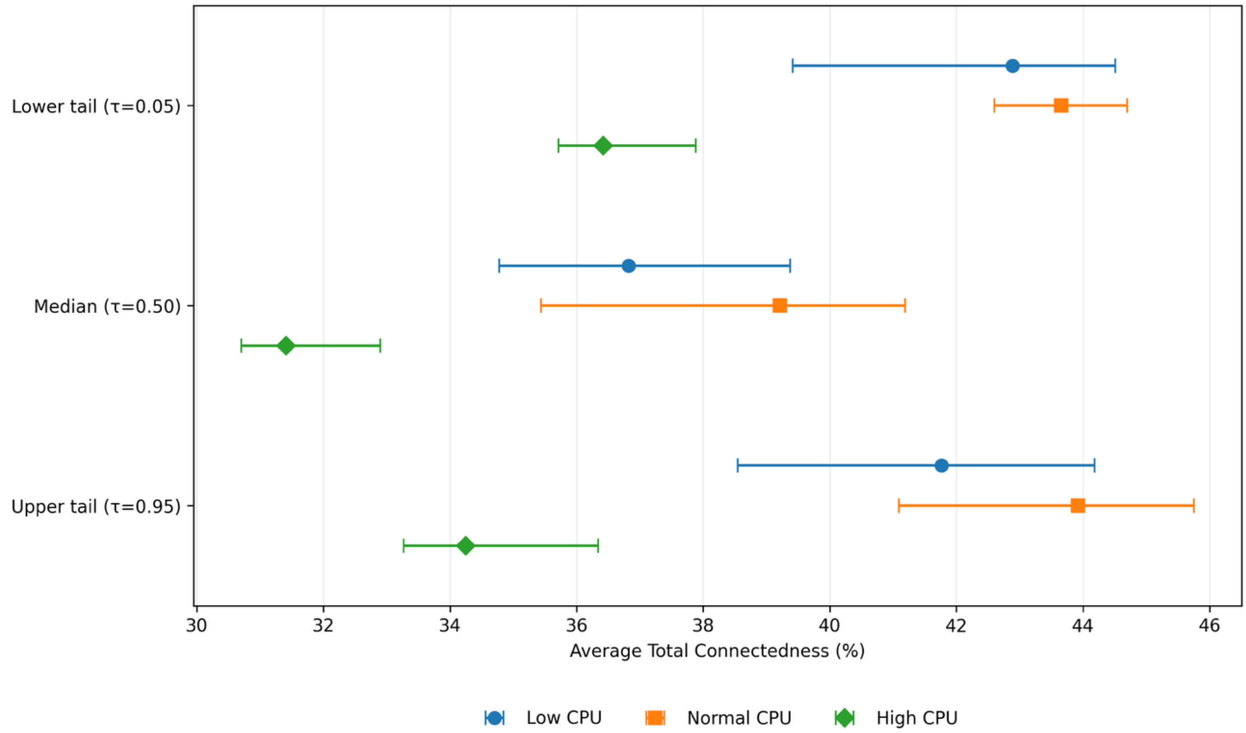

Fig 6. Total connectedness across CPU regimes and return quantiles

Note: The figure reports average total quantile connectedness under low-, normal-, and high-CPU regimes at $\tau = 0.05$, 0.50, and 0.95. Points represent regime-specific mean TCI and error bars denote 95% confidence intervals obtained from 1,000 moving-block bootstrap replications. CPU regimes are defined by the 33rd and 67th percentiles of logged CPU. QVAR estimates use a 200-day rolling window, one lag, and a 20-day forecast horizon.

The re-estimated confidence intervals are approximately 39.41–44.51, 42.60–44.70, and 35.71–37.88 for Low, Normal, and High CPU at the lower tail; 34.78–39.37, 35.44–41.19, and 30.70–32.90 at the median; and 38.54–44.18, 41.09–45.75, and 33.27–36.34 at the upper tail.

4.3.2. Network Composition across CPU Regimes

Aggregate TCI may conceal changes in the structure of spillovers. Figure 7 therefore compares net transmitter–receiver positions and pairwise directional connectedness across CPU regimes at the lower tail, median, and upper tail.

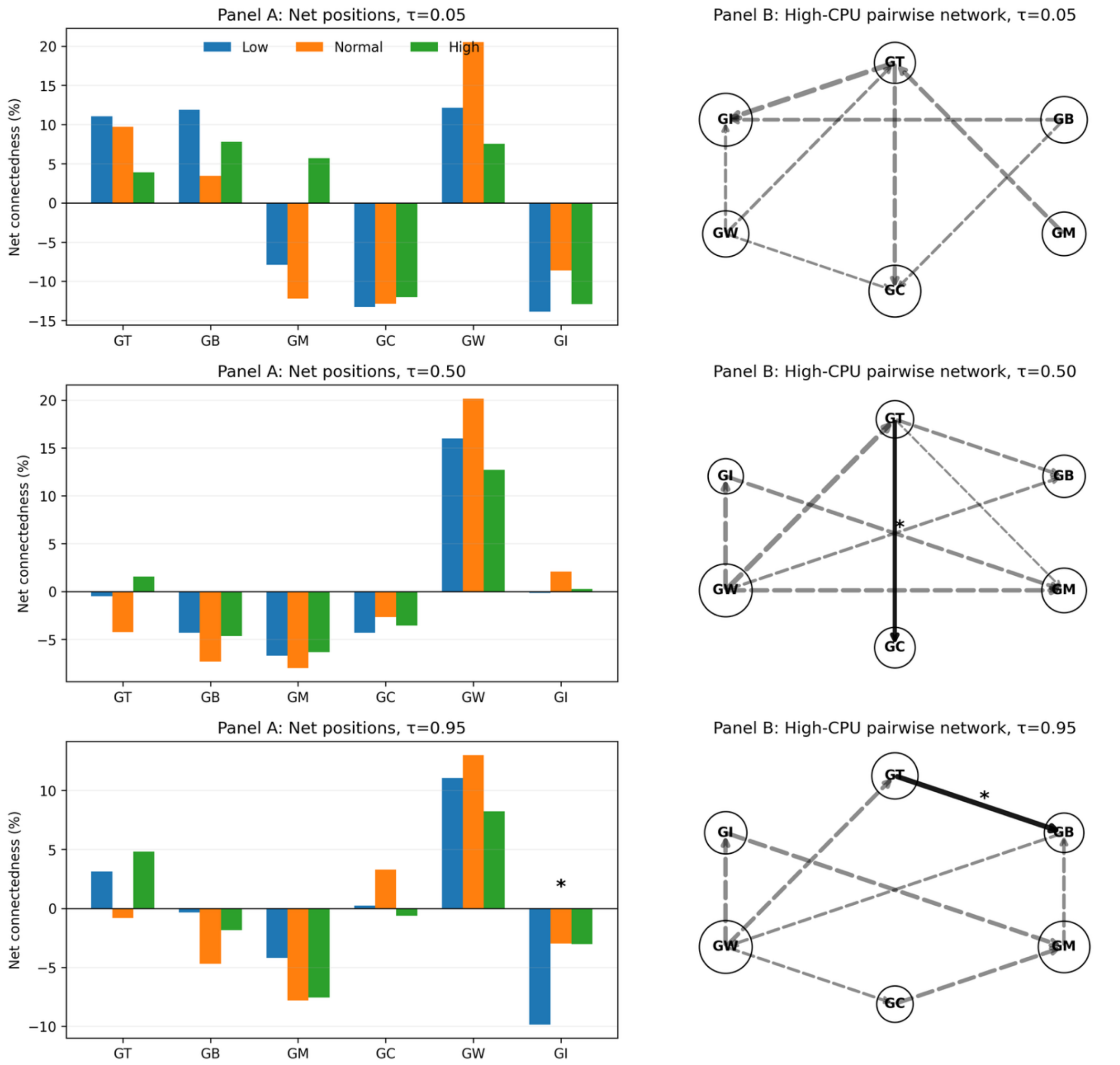

Figure 7. Green-Asset Network Composition across CPU Regimes

Note: Panel A reports average net directional connectedness for GT, GB, GM, GC, GW, and GI under low-, normal-, and high-CPU regimes at $\tau = 0.05$, 0.50, and 0.95. Positive values indicate net transmitters and negative values indicate net receivers. Panel B displays the strongest pairwise spillovers under high CPU; arrows indicate transmission direction and line thickness reflects spillover magnitude. Asterisks identify Low–High differences significant at the 5% level after Benjamini–Hochberg adjustment. Estimates use a 200-day rolling window, one lag, and a 20-day forecast horizon.

Figure 7 indicates that network roles vary across CPU regimes and quantiles. GW generally remains a net transmitter, while GC is more frequently positioned as a receiver. At the lower tail, GM shifts from a receiver under low CPU (−7.92) to a transmitter under high CPU (+5.70), although this change is not statistically significant after adjustment. The observed variation across regimes is broadly consistent with recent evidence that connectedness networks may differ across market states (Özkan et al., 2024; Wang et al., 2023).

More statistically supported changes appear at the median and upper tail. At the median, GT→GC strengthens, GB–GC reverses direction, and GW→GC weakens. In the upper tail, GI becomes a less pronounced net receiver, while GT→GB transmission strengthens. Table 6 summarizes these significant Low–High differences.

Table 6. Significant Changes in Net and Pairwise Connectedness between Low- and High-CPU Regimes

Quantile	Market	Low CPU	High CPU	High–Low difference	Adjusted p-value	Change
0.50	GT → GC	1.673	2.909	+1.237	0.014	Strengthened
0.50	GB–GC	−0.164	+0.545	+0.709	0.010	Direction reversal
0.50	GW → GC	1.796	0.599	−1.197	0.010	Weakened
0.95	GI net connectedness	−9.864	−3.038	+6.825	0.021	Receiver position weakened
0.95	GT → GB	0.860	4.251	+3.391	0.021	Strengthened

Note: The table reports Low–High differences significant at the 5% level after Benjamini–Hochberg adjustment. Pairwise values represent net directional transmission in the indicated direction. Negative net connectedness denotes a receiver and positive values denote a transmitter. P-values are based on 1,000 moving-block bootstrap replications.

Significant differences are concentrated at the median and upper tail. High CPU is associated with stronger GT→GC and GT→GB transmission, weaker GW→GC transmission, and a less negative GI position. Together with the lower aggregate TCI reported in Table 5, these patterns are consistent with network reconfiguration rather than a uniform weakening of spillovers under high CPU.

4.4. Robustness Tests

Table 7 evaluates the regime results using alternative rolling windows, forecast horizons, CPU classifications, and a mean-based generalized connectedness specification. The negative High–Low relationship is retained in most specifications, although the 150-day window produces a different tail pattern.

Table 7. Robustness of CPU-Regime Connectedness Differences

Specification	Lower-tail High–Low	Median High–Low	Upper-tail High–Low	Main conclusion retained?
Baseline: 200-day, H=20	−6.465	−5.413	−7.511	Yes
150-day window	+4.210	−0.030	+1.342	No
250-day window	−0.106	−0.457	−1.707	Yes
Forecast horizon H=10	−5.635	−5.413	−7.514	Yes
Two CPU regimes (median split)	−3.682	−1.191	−2.871	Yes
Mean-based generalized connectedness	—	−5.584	—	Yes

Note: Entries report the High–Low CPU difference in average total connectedness. Alternative rolling windows use 150 and 250 observations relative to the 200-day baseline. The alternative horizon uses $H = 10$, while the two-regime specification classifies observations using median logged CPU. Mean-based generalized connectedness provides a conventional mean-based comparison with the median QVAR result.

The negative High–Low difference remains under the 250-day window, shorter forecast horizon, median CPU split, and mean-based specification. The 150-day window differs, with positive tail differences and an approximately zero median difference. The baseline finding is therefore generally robust but sensitive to shorter rolling-window estimation, particularly in the distributional tails.

5. Conclusion

This study examines whether green-related market connectedness differs across low-, normal, and high-climate policy uncertainty (CPU) regimes using a quantile connectedness framework. The full-sample analysis indicates stronger connectedness in the lower and upper tails than around the median, together with heterogeneous transmitter–receiver roles across markets.

The regime analysis suggests that total connectedness is lower under high CPU than under low CPU across the three benchmark quantiles, while normal CPU records the highest average connectedness. The results also indicate that changes in aggregate connectedness are accompanied by changes in network composition. Several markets exhibit different transmitter–receiver roles across regimes, and selected bilateral spillovers strengthen, weaken, or reverse direction. These findings suggest that differences in aggregate connectedness may coincide with changes in the structure of spillover transmission.

The robustness analysis generally preserves the direction of the High–Low regime differences under alternative rolling windows, forecast horizons, CPU classifications, and mean-based connectedness, although some sensitivity is observed for the shorter rolling-window specification.

Overall, the findings complement recent evidence that climate policy uncertainty is associated with connectedness and risk transmission across sustainable financial markets (Özkan et al., 2024; Wang et al., 2023), while extending this literature by examining network reconfiguration across CPU regimes in addition to changes in aggregate connectedness.

The findings should be interpreted as conditional associations rather than causal relationships and remain subject to the selected model specification and asset coverage. Future research could examine alternative climate policy uncertainty measures, broader sets of green and transition-related assets, and whether the observed network reconfiguration remains consistent under different market conditions or connectedness frameworks.

References

Aastveit, K. A., Natvik, G. J., & Sola, S. (2017). Economic uncertainty and the influence of monetary policy. Journal of International Money and Finance, 76, 50–67.

Andersson, M., Bolton, P., & Samama, F. (2016). Hedging climate risk. *Financial Analysts Journal*, *72*(3), 13-32.

Ando, T., Greenwood-Nimmo, M., & Shin, Y. (2022). Quantile Connectedness: Modeling Tail Behavior in the Topology of Financial Networks. Management Science, 68(4), 2401–2431.

Andrews, D. W. K. (1993). Tests for Parameter Instability and Structural Change With Unknown Change Point. Econometrica, 61(4), 821–856.

Ang, A., & Bekaert, G. (2002). International asset allocation with regime shifts. The review of financial studies, 15(4), 1137-1187.

Antonakakis, N., Chatziantoniou, I., & Gabauer, D. (2020). Refined measures of dynamic connectedness based on time-varying parameter vector autoregressions. Journal of Risk and Financial Management, 13(4), 84.

Arfaoui, N., Naeem, M. A., Maherzi, T., & Kayani, U. N. (2024). Can green investment funds hedge climate risk?. *Finance Research Letters*, *60*, 104961.

Arif, M., Naeem, M. A., Farid, S., Nepal, R., & Jamasb, T. (2022). Diversifier or more? Hedge and safe haven properties of green bonds during COVID-19. Energy Policy, 168, 113102.

Ayed, S., Ben-Amar, W., & Arouri, M. (2024). Climate policy uncertainty and corporate dividends. Finance Research Letters, 60, 104948.

Azimli, A. (2022). The impact of policy, political and economic uncertainty on corporate capital investment in the emerging markets of Eastern Europe and Turkey. Economic Systems, 46(2), 100974.

Azimli, A. (2023). The impact of climate policy uncertainty on firm value: Does corporate social responsibility engagement matter?. Finance Research Letters, 51, 103456.

Azimli, A., & Cek, K. (2024). Can sustainability performance mitigate the negative effect of policy uncertainty on the firm valuation? Sustainability Accounting, Management and Policy Journal, 15(3), 752-775.

Baker, S. R., Bloom, N., and Davis, S. J. (2016). Measuring economic policy uncertainty. The Quarterly Journal of Economics, 131(4):1593–1636.

Bernanke, B. S. (1983). Irreversibility, Uncertainty, and Cyclical Investment. The Quarterly Journal of Economics, 98(1), 85–106.

Bolton, P., & Kacperczyk, M. (2021). Do investors care about carbon risk?. *Journal of financial economics*, *142*(2), 517-549.

Bouri, E., Iqbal, N., & Klein, T. (2022). Climate policy uncertainty and the price dynamics of green and brown energy stocks. Finance Research Letters, 47, 102740.

Broock, W. A., Scheinkman, J. A., Dechert, W. D., & LeBaron, B. (1996). A test for independence based on the correlation dimension. Econometric Reviews, 15(3), 197–235.

Bua, G., Kapp, D., Ramella, F., & Rognone, L. (2024). Transition versus physical climate risk pricing in European financial markets: A text-based approach. *The European Journal of Finance*, *30*(17), 2076-2110.

Cepni, O., Demirer, R., & Rognone, L. (2022). Hedging climate risks with green assets. Economics Letters, 212, 110312.

Chatziantoniou, I., Abakah, E. J. A., Gabauer, D., & Tiwari, A. K. (2022). Quantile time–frequency price connectedness between green bond, green equity, sustainable investments and clean energy markets. Journal of Cleaner Production, 361, 132088.

Chatziantoniou, I., Gabauer, D., & Stenfors, A. (2021). Interest rate swaps and the transmission mechanism of monetary policy: A quantile connectedness approach. Economics Letters, 204, 109891.

Chenet, H., Ryan-Collins, J., & Van Lerven, F. (2021). Finance, climate-change and radical uncertainty: Towards a precautionary approach to financial policy. Ecological Economics, 183, 106957.

Dickey, D. A., & Fuller, W. A. (1979). Distribution of the Estimators for Autoregressive Time Series With a Unit Root. Journal of the American Statistical Association, 74(366), 427–431.

Diebold, F. X., & Yilmaz, K. (2012). Better to give than to receive: Predictive directional measurement of volatility spillovers. International Journal of Forecasting, 28(1), 57–66. https://doi.org/10.1016/j.ijforecast.2011.02.006

Du, Y., & Guo, Q. (2023). Green credit policy and green innovation in green industries: Does climate policy uncertainty matter?. Finance Research Letters, 58, 104512.

Dutta, A., Bouri, E., Rothovius, T., & Uddin, G. S. (2023). Climate risk and green investments: New evidence. *Energy*, *265*, 126376.

Engle, R. F., Giglio, S., Kelly, B., Lee, H., & Stroebel, J. (2020). Hedging climate change news. *The Review of Financial Studies*, *33*(3), 1184-1216.

Fisher, T. J., & Gallagher, C. M. (2012). New Weighted Portmanteau Statistics for Time Series Goodness of Fit Testing. Journal of the American Statistical Association, 107(498), 777–787.

Fuss, S., Szolgayova, J., Obersteiner, M., & Gusti, M. (2008). Investment under market and climate policy uncertainty. Applied Energy, 85(8), 708–721.

Gabauer, D., Chatziantoniou, I., & Stenfors, A. (2023). Model-free connectedness measures. Finance Research Letters, 54, 103804.

Gavriilidis, K. (2021). Measuring Climate Policy Uncertainty (SSRN Scholarly Paper 3847388).

Gulen, H., & Ion, M. (2016). Policy uncertainty and corporate investment. The Review of Financial Studies, 29(3), 523-564.

Hanif, W., Hernandez, J. A., Mensi, W., Kang, S. H., Uddin, G. S., & Yoon, S. M. (2021). Nonlinear dependence and connectedness between clean/renewable energy sector equity and European emission allowance prices. Energy Economics, 101, 105409.

Hansen, B. E. (1997). Approximate Asymptotic P Values for StructuraS-Change Tests. Journal of Business & Economic Statistics, 15(1), 60–67.

Hoque, M. E., Soo-Wah, L., & Billah, M. (2023). Time-frequency connectedness and spillover among carbon, climate, and energy futures: Determinants and portfolio risk management implications. Energy Economics, 127, 107034.

Huynh, T. D., & Xia, Y. (2021). Climate change news risk and corporate bond returns. Journal of Financial and Quantitative Analysis, 56(6), 1985-2009.

Ilhan, E., Sautner, Z., & Vilkov, G. (2021). Carbon tail risk. The Review of Financial Studies, 34(3), 1540-1571.

INV. (2023). Investing.Com.—Stock Market Quotes & Financial News. Retrieved September 12, 2023, from https://www.investing.com/

Jarque, C. M., & Bera, A. K. (1980). Efficient tests for normality, homoscedasticity and serial independence of regression residuals. Economics Letters, 6(3), 255–259.

Jin, D., & Yu, J. (2023). Predicting cryptocurrency market volatility: Novel evidence from climate policy uncertainty. *Finance Research Letters*, *58*, 104520.

Jin, J., Han, L., Wu, L., & Zeng, H. (2020). The hedging effect of green bonds on carbon market risk. International Review of Financial Analysis, 71, 101509.

Karim, S., Naeem, M. A., Shafiullah, M., Lucey, B. M., & Ashraf, S. (2023). Asymmetric relationship between climate policy uncertainty and energy metals: Evidence from cross-quantilogram. Finance Research Letters, 54, 103728.

Khan, S., Rehman, M. Z., Shahzad, M. R., Khan, N. U., & Abdul Razak, L. (2023). How prone are emerging markets' sectoral indices to global uncertainties? Evidence from the quantile connectedness approach with portfolio implications. International Journal of Emerging Markets.

Koop, G., Pesaran, M. H., & Potter, S. M. (1996). Impulse response analysis in nonlinear multivariate models. Journal of Econometrics, 74(1), 119–147.

Liu, N., Liu, C., Da, B., Zhang, T., & Guan, F. (2021). Dependence and risk spillovers between green bonds and clean energy markets. Journal of Cleaner Production, 279, 123595.

Londono, J. M. (2019). Bad bad contagion. Journal of Banking & Finance, 108, 105652.

Mandaci, P. E., Azimli, A., & Mandaci, N. (2023). The impact of geopolitical risks on connectedness among natural resource commodities: A quantile vector autoregressive approach. Resources Policy, 85, 103957.

McDonald, R. and Siegel, D. (1986). The value of waiting to invest. The Quarterly Journal of Economics, 101(4):707–728.

Mensi, W., Naeem, M. A., Vo, X. V., & Kang, S. H. (2022). Dynamic and frequency spillovers between green bonds, oil and G7 stock markets: Implications for risk management. Economic Analysis and Policy, 73, 331-344.

Naeem, M. A., Bouri, E., Costa, M. D., Naifar, N., & Shahzad, S. J. H. (2021). Energy markets and green bonds: A tail dependence analysis with time-varying optimal copulas and portfolio implications. Resources Policy, 74, 102418.

Naeem, M. A., Karim, S., & Tiwari, A. K. (2023). Risk connectedness between green and conventional assets with portfolio implications. Computational Economics, 62(2), 609-637.

Naeem, M. A., Karim, S., Abrar, A., Yarovaya, L., & Shah, A. A. (2023). Non-linear relationship between oil and cryptocurrencies: Evidence from returns and shocks. International Review of Financial Analysis, 89, 102769.

Naeem, M. A., Pham, L., Senthilkumar, A., & Karim, S. (2022). Oil shocks and BRIC markets: Evidence from extreme quantile approach. Energy Economics, 108, 105932.

Naeem, M. A., Sadorsky, P., & Karim, S. (2023). Sailing across climate-friendly bonds and clean energy stocks: An asymmetric analysis with the Gulf Cooperation Council Stock markets. Energy Economics, 126, 106911.

Ndubuisi, G., & Urom, C. (2023). Dependence and risk spillovers among clean cryptocurrencies prices and media environmental attention. Research in International Business and Finance, 65, 101953.

Niu, S., Zhang, J., Luo, R., & Feng, Y. (2023). How does climate policy uncertainty affect green technology innovation at the corporate level? New evidence from China. Environmental Research, 237, 117003.

Olasehinde-Williams, G., & Özkan, O. (2023). A consideration of the environmental externality of Turkey's integration into global value chains: Evidence from dynamic ARDL simulation model. Environmental Science and Pollution Research, 30(11), 29154–29163.

Ongsakul, V., Papangkorn, S., & Jiraporn, P. (2023). Estimating the effect of climate change exposure on firm value using climate policy uncertainty: A text-based approach. Journal of Behavioral and Experimental Finance, 40, 100842.

Özkan, O., Adebayo, T. S., & Usman, O. (2024). Dynamic connectedness of clean energy markets, green markets, and sustainable markets: the role of climate policy uncertainty. *Energy*, *303*, 131957.

Pástor, Ľ., Stambaugh, R. F., & Taylor, L. A. (2021). Sustainable investing in equilibrium. Journal of Financial Economics, 142(2), 550-571.

Pesaran, H. H., & Shin, Y. (1998). Generalized impulse response analysis in linear multivariate models. Economics Letters, 58(1), 17–29.

Phillips, P. C. B., & Perron, P. (1988). Testing for a Unit Root in Time Series Regression. Biometrika, 75(2), 335–346.

Rehman, M. Z., Khan, S., Khan, U. A., Alonazi, W. B., & Noman, A. A. (2023). How Do Global Uncertainties Spillovers Affect Leading Renewable Energy Indices? Evidence from the Network Connectedness Approach. Sustainability, 15(18), 13630.

Rubtsov, A., Xu, W., Šević, A., & Šević, Ž. (2021). Price of climate risk hedging under uncertainty. Technological Forecasting and Social Change, 165, 120430.

S&P DJI. (2023). S&P Dow Jones Indices. Retrieved September 11, 2023, from https://www.spglobal.com/spdji/en/

Salisu, A. A., & Vo, X. V. (2020). Predicting stock returns in the presence of COVID-19 pandemic: The role of health news. International Review of Financial Analysis, 71, 101546.

Shahbaz, M., Sheikh, U. A., Tabash, M. I., & Jiao, Z. (2024). Shock transmission between climate policy uncertainty, financial stress indicators, oil price uncertainty and industrial metal volatility: Identifying moderators, hedgers and shock transmitters. *Energy Economics*, *136*, 107732.

Sun, G., Fang, J., Li, T., & Ai, Y. (2024). Effects of climate policy uncertainty on green innovation in Chinese enterprises. International Review of Financial Analysis, 91, 102960.

Tiwari, A. K., Abakah, E. J. A., Gabauer, D., & Dwumfour, R. A. (2022). Dynamic spillover effects among green bond, renewable energy stocks and carbon markets during COVID-19 pandemic: Implications for hedging and investments strategies. Global Finance Journal, 51, 100692.

Tiwari, A. K., Abakah, E. J. A., Rehman, M. Z., & Lee, C.-C. (2023). Quantile dependence of Bitcoin with clean and renewable energy stocks: New global evidence. Applied Economics, 0(0), 1–15.

Tiwari, A. K., Trabelsi, N., Abakah, E. J. A., Nasreen, S., & Lee, C.-C. (2023). An empirical analysis of the dynamic relationship between clean and dirty energy markets. Energy Economics, 124, 106766.

Treepongkaruna, S., Chan, K. F., & Malik, I. (2023). Climate policy uncertainty and the cross-section of stock returns. Finance Research Letters, 55, 103837.

Urom, C. (2023). Time–frequency dependence and connectedness between financial technology and green assets. *International Economics*, *175*, 139-157.

Vo, H., Nguyen, T., & Phan, H. V. (2024). Building a sustainable future: The role of corporate social responsibility in climate policy uncertainty management. Finance Research Letters, 60, 104831.

Wang, K. H., Wang, Z. S., Yunis, M., & Kchouri, B. (2023). Spillovers and connectedness among climate policy uncertainty, energy, green bond and carbon markets: A global perspective. Energy Economics, 128, 107170.

Wang, X., Li, J., & Ren, X. (2022). Asymmetric causality of economic policy uncertainty and oil volatility index on time-varying nexus of the clean energy, carbon and green bond. International Review of Financial Analysis, 83, 102306.

Wang, Y., Bouri, E., Fareed, Z., & Dai, Y. (2022). Geopolitical risk and the systemic risk in the commodity markets under the war in Ukraine. Finance Research Letters, 49, 103066.

Zhang, J., Chen, X., Wei, Y., & Bai, L. (2023). Does the connectedness among fossil energy returns matter for renewable energy stock returns? Fresh insights from the Cross-Quantilogram analysis. International Review of Financial Analysis, 88, 102659.

Zhang, Y., & Umair, M. (2023). Examining the interconnectedness of green finance: an analysis of dynamic spillover effects among green bonds, renewable energy, and carbon markets. Environmental Science and Pollution Research, 1-17.